ISSN NO. 2320-5407

*Journal homepage: http://www.journalijar.com*

*INTERNATIONAL JOURNAL OF ADVANCED RESEARCH*

**RESEARCH ARTICLE**

# Epoxy/silica nanocomposites and benefit of a gelatin interface on nanocomposite properties

**Abdelrahman Mohamed[1,2], Soha M. Albukhari[1,3], Hisham Essawy[4], Ahmed H.H. EL-Ghandour[2], Sayed A. Ahmed[2], Patricia A. Heiden[1]**

**1.** Department of Chemistry, Michigan Technological University, Houghton, MI, 49931 USA
**2.** Chemistry Department, Faculty of Science, Beni Suef University, Beni Suef, Egypt
**3.** Department of Chemistry, King Abdulaziz University, Jeddah, Saudi Arabia
**4.** Polymers & Pigments Department, National Research Center, Cairo- Egypt

## *Manuscript Info*

***Manuscript History:***

Received: 15 September 2014
Final Accepted: 26 October 2014
Published Online: November 2014

***Key words:***

***Corresponding Author***

**Abdelrahman Mohamed**

## *Abstract*

Strong interfacial adhesion between phases is needed for most effective enhancement of mechanical properties. Epoxies reinforced with silica microparticles is well studied, but silica nanoparticle-reinforced studies are fewer, and many of those used commercial-grade surface-modified silica nanoparticles commercially available since 2002. Those nanoparticles appear to rely on silanol groups for bonding, but only small increases in tensile modulus, even at high nanoparticle loading, are found. Silica nanoparticles (ca. 20 nm) prepared in the presence of gelatin yield amine-rich surfaces. When added at 3 wt% to epoxy a 127% increase in tensile modulus was found. Composite fracture surfaces show generally uniform, nanoparticles (ca. 20 nm) but with occasional aggregates (ca. 100-250 nm). SEM showed many features that are associated with increased toughness but no particle cavities indicating excellent interfacial adhesion. Silica nanoparticles with amine-rich surfaces may be superior to silanol surfaces for interfacial bonding, and can be achieved using low-cost gelatin.



## Introduction

The development of polymeric materials with improved performance often relies upon the design and use of different additives. Over the last decade or so, the study and use of polymers containing nanosized fillers has been a major area of activity in pursuit of new materials. These nanocomposites often possess higher properties when compared to similar materials with macroscale fillers. These higher properties are attributed to the dramatic increase in the interfacial area.

Some examples of nanoscale additives include alumina trihydrate to impart fire retardancy, iron oxides for magnetic properties, and zinc oxide to produce materials exhibiting a non-linear resistivity.[1] All of these applications take advantage of enhanced surface area to achieve enhanced activity, just as catalysts do. When the nanoscale additive is intended as reinforcement for the matrix increased surface area alone is not sufficient to achieve the best property enhancement from the additive.

The property enhancement obtained in composite materials from an additive depends on composition, quantity, dimensions, filler shape, and the nature of the interface. [2] To function as reinforcement the additive must be able to accept loads transferred from the matrix, and this requires interfacial adhesion. Although even reinforcements that rely solely on van der Waals interactions can be beneficial at the nanoscale simply because of the extent of the surface area that can interact with the matrix, a more effective degree of interaction between reinforcements and matrix should yield greater enhancements in mechanical properties.[3,4]

Therefore, while surface treatments of nanoscale additives are often performed to minimize the formation of agglomerates during processing, if these additives are intended as reinforcement then the surface treatments can also be designed to enhance interfacial adhesion to the matrix to aid enhancement of mechanical properties[1]. Therefore, the use of functionalized nanoparticles can lead to a significant improvement of the mechanical properties of the composite materials.

Silica particles have long history of use as composite fillers for improving mechanical properties, particularly strength and modulus. This interest of course continues now with silica nanoparticles, which have been available commercially for more than a decade.[5] The silica surfaces can be easily modified to enhance interfacial adhesion, may already be able to bond to epoxy via the silanol groups, and additional surface modification may not be needed, but they are also frequently surface modified.[6,7]

The use of surface-modified silica nanoparticles has been reported to increase the cyclic fatigue resistance of the epoxy polymer [8, 9] and to afford only a small increase in the viscosity of the epoxy prepolymer.[10] Silica nanoparticles are often surface-modified by functional silanes, placing amines[11], or epoxide groups on the surface.[9] The use of aminoalkoxysilanes is a well-established and effective method for placing amines on silica surfaces[11], but amino silanes are expensive.

Instead of functionalizing silica nanoparticles after their preparation, we opted for a simple one-pot approach in which silica nanoparticles were prepared in the presence of gelatin, an inexpensive, abundant, and water-soluble natural polymer with numerous functional groups, e.g. carboxylic acids, alcohols, phenols, and amine groups. The gelatin is intended to control particle growth and prevent aggregation during sol-gel synthesis of the nanoparticles, while producing silica nanoparticles with highly functionalized gelatin shells. These functional groups can form covalent and hydrogen bonds and with many different matrices, including epoxy resins.

Here, we investigated the effects of preparation conditions on the size and stability of the silica core-gelatin shell nanoparticles, and their effects on the mechanical properties of a bisphenol-A type epoxy resin when they were added at 1, 3, and 5 wt%. We elected to test the ability of these nanoparticles to enhance the modulus of a low-temperature cured epoxy resin, rather than the more commonly researched high-temperature-cured epoxies, because of the potential advantage of gaining higher properties while saving cost from lower energy use and lower cost modifications.

## 2-EXPERIMENTAL

### 2.1. Materials

Gelatin (Type A, 300 Bloom), tetraethylorthosilicate (TEOS, Aldrich), ammonium hydroxide ($NH_4OH$, Aldrich) were used as received without further purification. D.E.R. 331, a bisphenol A based (DGEBA) epoxy resin with an Epoxide Equivalent Weight (EEW) of 182-192, and D.E.H. 29 cure agent/hardener, a complex mixture of linear, branched and cyclic amines, were kindly provided by Dow Chemical Company, and were used as received.

### 2.2. Preparation of silica/gelatin core-shell nanoparticles

Silica core-gelatin shell nanoparticles were prepared by dissolving 0.05 g gelatin in 10 mL deionized water at 40 ˚C under magnetic stirring for 10 minutes to reach the complete dissolution of the polymer. Then TEOS (0.90 mL, 0.84 g) was added to the gelatin solution with vigorous magnetic stirring followed by addition of $NH_4OH_{(aq)}$ (2 mL). The system was stirred at 20 ˚C over night. After evaporation of the solvent under reduced pressure (6 h at 40 °C), the silica/gelatin nanoparticles were obtained as a hygroscopic solid with $d_H$< 250 nm. Core-shell nanoparticles made by this route ($d_H$ < 250 nm) were used in all further work.

The above reaction conditions were repeated but with overnight stirring at 50 ˚C or at 80 ˚C, but the resulting nanoparticles possessed $d_H \geq 400$ nm. Other nanoparticle preparation conditions were also tested, and used higher concentrations of gelatin and TEOS (e.g. 3.5 mL TEOS and 0.5 g gelatin in 25 mL deionized water) with differing reaction temperatures, and some reactions tested acidic catalysts, but these all yielded nanoparticles with $d_H$ >350 nm.

### 2.3. Preparation of nanocomposites

Silica/gelatin nanoparticles were blended into the epoxy prepolymer (nanoparticle loading of 1, 3, and 5% by weight) were prepared by preheating the epoxy at 40-50 °C, and then adding the desired amount of silica/gelatin particles. This blend was sonicated in an ultrasonic bath for 0.5 h. After degassing under vacuum, the D.E.H. 29 hardener was added (15 wt %), and the system was cast into a silicon rubber mold with dog bone cavities. This mold was then placed between two metal plates to produce specimens having dimensions of 70 mm x 10 mm x 4 mm. The cure cycle recommended by the manufacturer for D.E.R. 331 with the highly reactive D.E.H. 29 hardener was 100 °C/2h but these nanocomposites, as well as the unmodified epoxy control, were cured at 100 ˚C/3.5 h.

### 2.4. Characterizations

Fourier transform infra-red (FTIR) spectra were taken on a Perkin–Elmer Spectrum One FTIR Spectrometer from 4000 to 650 $cm^{-1}$ (4.0 $cm^{-1}$ resolution). The hydrodynamic diameter of the silica/gelatin nanoparticles was determined in aqueous suspension by dynamic light scattering (Coulter NP4 Plus, Beckman Coulter, Fullerton, CA). An MTS universal testing machine was used to test the mechanical properties of the epoxy control and nanocomposite specimens. The reported results are the average of 5-6 test specimens. The fracture surfaces of these test specimens were observed by FESEM (Hitachi S-4700) under an acceleration voltage of 15 kV.

## 3-Results and Discussion

### 3.1. Nanoparticle preparation and characterization

The rationale for using silica core/gelatin shell nanoparticles as epoxy reinforcement is that silica is perhaps the most abundantly used epoxy filler, and, from prior research, we knew the gelatin was effective at aiding in the preparation of metal oxides nanoparticles prepared by sol-gel methods from metal alkoxides.[12] Furthermore, the low cost of gelatin with its high degree of functionality (carboxylic acids, alcohols, phenols, and amines) allows this inexpensive biopolymer to chemically bond to both the silica and numerous polymer matrices, including epoxies. Preparing the silica nanoparticles in the presence of a small amount of gelatin afforded uniform, spherical, and extremely small (ca. 10-20 nm Fig.1) nanoparticles, giving an approximate surface area between ca. $2.24\times10^{20}$ – $8.97\times10^{20}$ $nm^2/g$. These nanoparticles also appear to be uniformly distributed throughout the epoxy, though some micrographs show some nanoparticles formed larger aggregates of ca. 100-200 nm. These aggregates are not seen in most of the micrographs, but are present and so the micrographs shown in this paper were all selected to show the aggregates.

When the nanoparticle size was measured in aqueous suspension, using DLS, the hydrodynamic diameter ($d_H$) was greater than 200 nm, and depended on the temperature of the sol-gel reaction, as shown in Table 1. The hydrodynamic diameter ($d_H$) of the particles decreased with reaction temperature, showing the effect of collapse of the gelatin shell, but also suggesting that, even at the low end of the concentration range tested, some fraction of the gelatin-silica nanoparticles are present in the aqueous phase and the soluble gelatin can promote some degree of aggregation. This is inferred because the gelatin-silica nanoparticles' average $d_H$ was 228 nm at 20 ˚C, which is significantly larger than the observed particle size in SEM micrographs of dried particles, indicating an expanded and partially aggregated gelatin shell in the aqueous phase. The $d_H$ of particles made at higher temperatures are much higher and at 80 ˚C rose to ~1000 nm. This is expected given that gelatin is highly water-soluble but at 80 ˚C gels, allowing the silica nanoparticles to readily aggregate. It also shows the importance of using as little gelatin as needed to give the silica a dynamic reactive surface.

We experimented with higher concentrations of gelatin and TEOS in the sol-gel synthesis but all the conditions tested resulted in $d_H$ > 350 nm. SEMs were not taken of the hybrid nanoparticles prepared under these conditions, and none of these were used in composites. Therefore, the actual size of the silica domains formed under these other conditions is unknown, but we hypothesize that the number and size of aggregates in the composites would be greater when using more gelatin in their preparation.

We also wanted to confirm the availability of functional groups, and in particular amine groups, on the surface of the hybrid nanoparticles because we expect these groups to readily form covalent bonds to the epoxy thermoset. As stated previously, forming a strong interface to the matrix is critical for effective reinforcement, and forming covalent bonds to the epoxy should achieve significant mechanical property enhancement in the composite. The FTIR spectrum of the silica/gelatin nanoparticles is seen in Fig. 2a. A strong band is seen around 3350 $cm^{-1}$

corresponding to N-H stretching vibration, and possibly some O–H vibrations also. The aliphatic C-H stretches from gelatin are not visible, but strong bands are observed at 1750 and 1500 $cm^{-1}$corresponding to amide vibrations, while a narrow peak at 1400 $cm^{-1}$ suggests the presence of carboxylate groups.[13] Amino as well as alkyl chains are evident in the band from 1200 to 1000 $cm^{-1}$. Bands characteristic of silica[14] are also clearly evident in the degenerated stretching and bending vibration modes of the [SiO4] tetrahedron at 1100 $cm^{-1}$, the Si–OH vibration at 945 $cm^{-1}$ and the Si–O–Si bending vibration mode at 800 $cm^{-1}$.

Fig. 2b shows the FTIR spectrum of an uncured epoxy composite containing 1 wt. % of the hybrid silica/gelatin nanoparticles but no cure agent. The most favored reaction between epoxy and silica/gelatin nanoparticles likely involves the epoxide with the primary amino groups of the gelatin shell. In the uncured epoxy-nanoparticle blend alkyl stretches, just below 3000 $cm^{-1}$, are observed and are attributed to those from the epoxy resin. The N-H band, at 3350 $cm^{-1}$, is no longer observed and the intensity of the silanol band at 975 $cm^{-1}$ is also decreased, indicating these groups appear to be reacting with the epoxy groups under the blending conditions. Furthermore, the peaks at 1519 and 1480 $cm^{-1}$, which correspond to the aromatic ring deformation modes of the epoxy monomer, support bonding to the silica particles.[15] Overall, the FTIR supports direct reaction between the epoxide and the gelatin N-H groups, but also the silanol groups of the silica core. The apparent reaction of the silanol groups suggests that the gelatin shell does not completely coat the silica core.

An FT-IR spectrum of the cured epoxy nanocomposite is not included because the large number of the D.E.H. 29 amines would obscure any reaction from the gelatin shell. Definitive proof of the reaction of the gelatin's functional groups was therefore not obtained here, since even if we showed that the gelatin bonded to epoxy in the absence of the cure agent, that would not prove its functionalities competed effectively with the D.E.H. amine groups. However, reaction between epoxide rings and gelatin N-H groups is demonstrated elsewhere.[16, 17]

The effective bonding of the gelatin shell to the epoxy is however also strongly supported by the SEM micrographs of the fracture surface of the composites shown in Fig. 1**.** There are no cavities seen in the composites from expulsion of a reinforcing phase which is typical of weak interfacial bonding between the matrix and the reinforcement, as is often observed in rubber-toughened epoxies.[18,19]

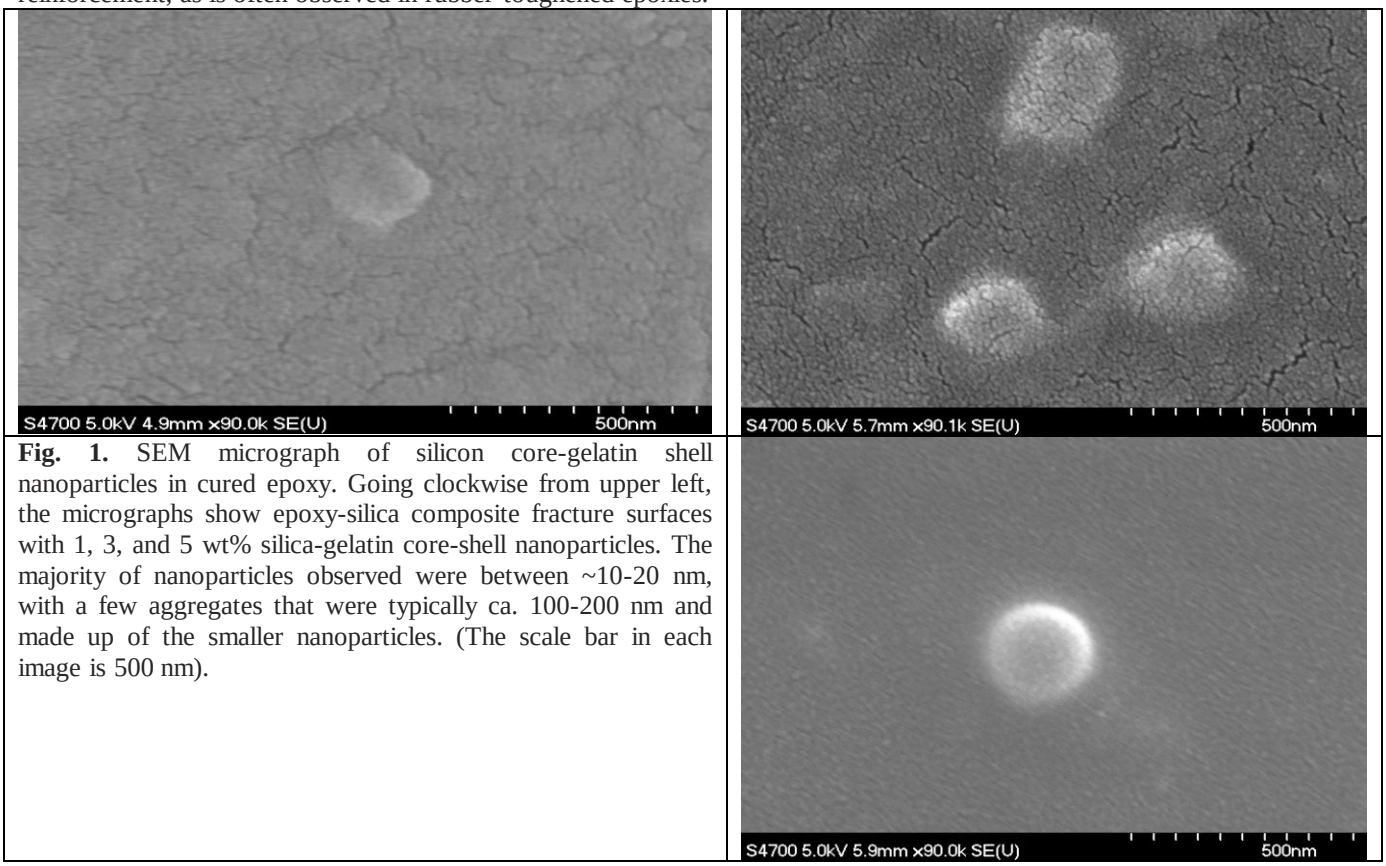


**Fig. 1.** SEM micrograph of silicon core-gelatin shell nanoparticles in cured epoxy. Going clockwise from upper left, the micrographs show epoxy-silica composite fracture surfaces with 1, 3, and 5 wt% silica-gelatin core-shell nanoparticles. The majority of nanoparticles observed were between ~10-20 nm, with a few aggregates that were typically ca. 100-200 nm and made up of the smaller nanoparticles. (The scale bar in each image is 500 nm).

Table 1. Hydrodynamic Diameter of Silica Core-Gelatin Shell Nanoparticles

| Temperature of Measurement | Average Hydrodynamic Diameter (nm) |
|---|---|
| 80 ˚C | 1000 |
| 40 ˚C | 400 |
| 20 ˚C | 228 |

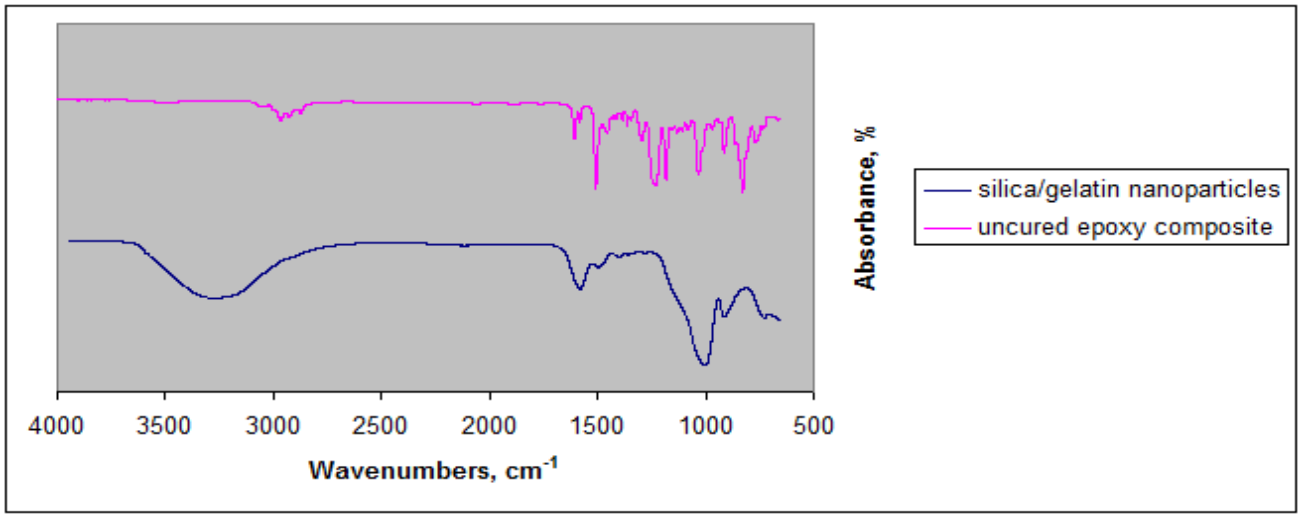


**Figure 2**. FT-IR of (a) silica/gelatin core-shell nanoparticles at bottom of figure, and (b) uncured epoxy composite containing 1 wt% silica/gelatin nanoparticles seen at top.

### 3.2. Mechanical properties of epoxy-silica nanocomposites

SEM analysis of the fracture surface of the epoxy nanocomposites showed a uniform dispersion of nano-sized particles that were mostly ca. 10-20 nm. This of course gives an ultra-large interfacial area per unit volume, calculated as 1256 $nm^2$ for an individual nanoparticle of 20 nm, and assuming a uniform distribution of 20 nm nanoparticles within the epoxy matrix, an estimated $2.58\times10^{17}$ , $7.74\times10^{17}$ and $12.9\times10^{17}$ $nm^2$ per unit volume, for 1, 3, and 5 wt.% respectively. This calculation does not take into account the aggregates within the matrix, which would lower that number.

The fracture toughness of the composites was not measured, but the SEM micrographs of the fracture surfaces shown in Fig. 1 prove a very strong interfacial adhesion between the silica nanoparticle reinforcement and matrix, and show several other features that strongly support a significant rise in toughness.

Other published reports of epoxy reinforced with silica nanoparticles of ca. 20 nm did report toughness increases. For example, Johnsen et *al.*[18] found significant increases in fracture toughness with silica nanoparticle-filled epoxy, even though their SEM micrographs showed numerous particle voids and other evidence of weak interfacial adhesion. However, it is well established that rough surfaces have the effect of increasing the true fracture surface area.[18] In our case, the strong interfacial adhesion is proven by the absence of particle cavity formation, which is routinely observed in composites with poor interfacial adhesion, e.g. rubber-toughened epoxies without adhesion promoters.[18] Although the particles continue to adhere strongly to the epoxy matrix, showing de-bonding at the particle-matrix interface is not involved in property improvements, an increased fracture toughness is supported by the rough surface resulting from the nearly continuous field of embedded 10-20 nm silica nanoparticles, giving requiring fracturing a higher surface area than the planar area would suggest (Fig. 1) which supports an increased fracture energy.

A rise in toughness is also inferred from the numerous crack deflections observed, where the cracks follow a path around the many 10-20 nm silica nanoparticles. When the crack propagates to a silica aggregate, rather than deflect

around these particles, paths form through the aggregate, as clearly seen in Fig. 1 with the 3 wt% silica nanoparticles. This indicates that the individual silica core-gelatin shell nanoparticles do not adhere as well to each another as they do the epoxy matrix. And, when the cracks propagate through the aggregate, they do so via a 'tortuous' pathway around the individual nanoparticles within the aggregate, and not as a brittle failure of the aggregate.

These observed features are well-established toughening mechanisms.[20] In fact, crack deflection is reported to be the major toughening mechanism from the incorporation of rigid microscale particles into brittle matrices[21,22] Two other reported modes of toughening in composites with rigid microscale reinforcements are plastic deformation,[22,23] and crack front pinning,[23,24] but while we cannot state definitively that these did not occur, they were not apparent in the SEM micrographs of our nanocomposites.

The tensile modulus was measured (Table 2) from the stress-strain curves (Figure 3). An increase in modulus is expected when epoxy is reinforced with silica since the modulus of silica itself is 70 GPa.[18] However, these composites showed a significant rise in modulus even at very low loading. A 1 wt % addition of silica nanoparticles leads to a 69 % increase in modulus, and at just 3 wt % the modulus rises by 127 %. When the silica loading is increased to 5 wt % the modulus is 118 % higher than the unreinforced epoxy control which is substantial but slightly less high than with 3 wt % loading.

Table 2. Increase in Tensile Modulus with Nanoparticle Loading

| Nanoparticle Loading in Epoxy (wt %) | Nanoparticle Volume % | Modulus (MPa) | % Increase |
|---|---|---|---|
| 0 | — | 1742.37±274 | — |
| 1 | 0.73 | 2949.97±210 | 69 |
| 3 | 2.2 | 3951.23±756 | 127 |
| 5 | 3.6 | 3793.47±624 | 118 |

These percentage increases are very impressive when compared with existing literature for epoxy resins reinforced with silica particles. For example, Johnsen et *al.*[18] using an anhydride-cured DEGBA based epoxy (EEW 185 g/mol) and achieved a 30 % increase with 20 wt % loading of silica nanoparticles that had a similar size to the ones used in this work, but with unknown surface properties. Rosso et *al.*[25] also used a DEGBA based epoxy (EEW not reported) and obtained approximately a 20 % increase in modulus using 5 vol. % of silica nanoparticles of ca. 50 nm with a surface modification described as giving a hydroxyl-rich surface.

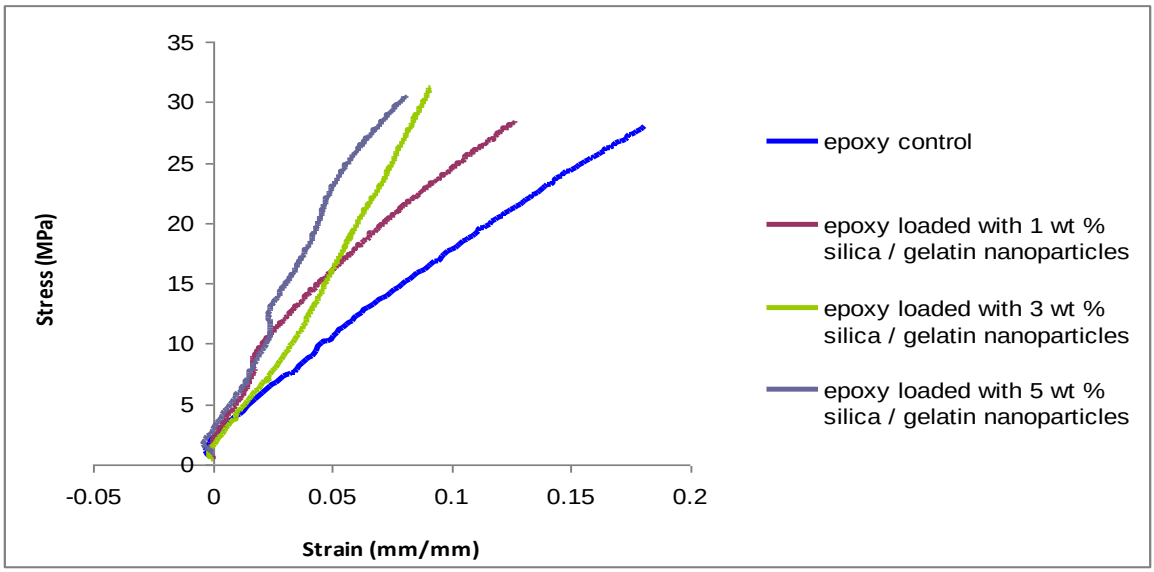

**Figure 3.** Stress-Strain curves for neat epoxy and epoxy nanocomposites.

Deng et *al.*[26] used various weight percentages of 20 nm silica nanoparticles in an aliphatic amine-cured DEGBA based epoxy resin (Araldite-F, EEW not reported) and found a maximum increase in tensile modulus of just 14 % when 8 wt % nanoparticles were added, and in a second study that measured modulus at elevated temperatures found no increase in modulus.[26] Also using aliphatic amine-cured DEGBA based epoxy resins Tsai et *al.* found a modulus increase of 19 % with 40 wt % silica loading while Ye et *al.* found a ca. 14 % rise in modulus with 10 wt % nanosilica.[7] Polyether amine curing agents also did not yield higher increases in modulus values using nanosilica reinforcement.[7]

The most noteworthy feature of these results is that the percent increase in the modulus of all of these silica-reinforced epoxy composites was considerably less than the percent increase we measured with a much lower silica loading, and this increase in modulus must be attributed to the amine interface of the nanosilica reinforcement. However, those epoxy resins were cured at high temperatures and were intended for higher temperature use, so they started with higher moduli than this resin. However, the typical modulus of DGEBA-based epoxies in those studies without reinforcement was ca. 3 GPa, versus the modulus of this epoxy was ca. 1.7 GPa, but still the silica modulus is ca. 70 GPa, so the effect of the amine interface afforded by gelatin still seems to be the key factor in the much higher modulus of these resins.

A recent review paper[7] surveyed the literature and plotted the rise in modulus of DGEBA epoxy resins cured with different hardeners (and at various temperatures consistent with those hardeners), as a function of nanosilica up to 23 wt %. The initial modulus of the DGEBA epoxies used in that review ranged from ca. 2.8-3.2 GPa, compared to our lower-temperature epoxy with an initial modulus of ca. 1.7 GPa. While the literature resins experienced a rise in modulus of only ca. 19 % at 10 wt % nanosilica loading and at 20 wt % nanosilica loading the moduli rose by only 40 % or less. Most of the epoxies at 20 wt% loading reached a maximum modulus in the range of ca. 3.5 – 3.8 GPa, compared to our DEGMA epoxy with 3 wt % nanosilica loading possessed a modulus of nearly 4 GPa. In the review paper only an epoxy cured with diaminodiphenylsulfone (DDS), a high temperature cure agent gave a higher modulus of ca. 4.5 GPa.

This further confirms that the significant effect in the modulus rise was the use of a gelatin (amine-rich) shell around the silica nanoparticles and the effect of the gelatin shell was the amine-rich interface affording a much stronger adhesion that the more commonly used silanol and –OH interfaces that appear to be commonly employed for interfacial adhesion. [5] While it is likely that a similar enhancement in interfacial bonding would be achieved with functionalizing silica nanoparticles with an aminosilanol species, those interfacial modifiers are far more expensive than gelatin.

Finally, while an epoxy beginning with a higher modulus may not give the same percent increase as was observed for low temperature/low modulus systems used here, the difference in interfacial adhesion seems to be the major factor in achieving the significant rise in modulus, and the modulus of even the highest modulus epoxy does not compare with that of silica itself. Therefore, a significant benefit from reinforcing high-modulus epoxies with amine-rich polymers should be expected.

## Conclusion

We showed that silica nanoparticles with gelatin-coated surfaces are achieved by a simple one-pot sol-gel method done in the presence of a small amount of gelatin, an extremely inexpensive natural polymer. These nanoparticles formed such strong interfacial interactions to epoxy that fracture surfaces showed no sign of particle cavitation, and increases in tensile modulus of 127 % were achieved with just 3 wt % loading of the gelatin-coated silica nanoparticles. This far exceeds any other value found in the literature for epoxy reinforced with other silica nanoparticles. We attribute this increase to the strong interfacial adhesion of the gelatin-modified silica nanoparticles, and in particular to the amine-groups of the gelatin. Aminosilanes are commonly used to impart amine surfaces to metal oxide nanoparticles like silica, but gelatin is far less costly, and has the added advantage of also possessing hydroxyl, phenolic, and carboxylic acid groups. Thus, a “single pot” product might be made that can also be used to reinforce other matrices that would benefit from these other groups. Fracture toughness was not measured but fracture surfaces showed numerous features that are associated with enhanced toughness. Using gelatin-coated silica nanoparticles has the potential to produce silica-reinforced epoxy thermosets at lower temperatures and with lower silica loadings and similar or superior moduli than the more-commonly used silica-

reinforced epoxy thermosets. Furthermore, this inexpensive modifier approach may open up opportunities to develop other composite materials with good potential in industrial applications.

## References

1) Kinloch, A.J., Shaw, S.J., Tod, D.A., and Hunston D.L. *Polymer* **1983**, 24, 1341-1354.

2) Nielsen, L. E., Landel, R. F. Mechanical Properties of Polymers and Composites; Marcel Dekker, Inc., New York, **1994**.

3) Zheng, Y. and Ning, R. Materials Letters, **2003**, 57, 2940-2944.

4) Jennifer, V., Delphine, D., Nelesh, P., Claudia, B., Serena, B., José, D. S., Maria, A. L., William, B., and Christine, O. Journal of Biomedical Materials Research Part A. **2006**, 78, 352-363.

5) Odegard, G.M., Clancy, T.C., and Gates, T.S. Polymer **2005**, 46, 553-562.

6) Bray, D.J., Dittanet, P., Guild, F.J., Kinloch, A.J., Masania, K., Pearson, R.A., and Taylor, A.C. Polymer. **2013**, 54, 7022-7032.

7) Sprenger, S. J. Appl. Poly Sci. **2013**, 1421-1428.

8) Hsieh, T.H., Kinloch, A.J., Masania, K., Sohn, Lee J., Taylor, A.C., and Sprenger, S. J. Mater. Sci. **2010**, 45, 1193-1210.

9) Rudiger, N., Thomas, S., and Rodney, C., Conn. Patent WO 2013156337 A1, Oct. 24, **2013**.

10) Roscher, C. Eur Coat J. **2003**, 4, 131-141.

11) Joong, H.M., JiWon, S., Sang, Y. K., and Joon, W. P. *Langmuir* **1996**, 12, 4621-4624.

12) Ken, H. S., Michael, E. M., Owen, P. M., and Patricia, A. Heiden. Nanotechnology **2005**, 16, 1950. *doi:10.1088/0957-4484/16/9/088*.

13) Socrates, G. Infrared Characteristic Group Frequencies: Tables and Charts, 2nd edition*; Wiley:* Chichester, **1994**.

14) François, F. Terra Nova, **1989**, 1, 267-273.

15) Ragosta, G., Abbate, M., Musto, P., Scarinzi, G., and Mascia L. Polymer **2005**, 46, 10506–10516.

16) Meng, Z., Yuanjuan, W., Qingsi, Z., Yongmei, X., and Tianduo, L. *J. Appl. Polym*. Sci. **2011**, 120, 2130–2137.

17) Vargas, G., Acevedo, J.L., López, J., and Romero, J. *Materials Letters* **2008**, 62, 3656–3658.

18) Johnsen, B.B., Kinloch, A.J., Mohammed, R.D., Taylor, A.C., and Sprenger, S. *Polymer* **2007**, 48, 530-541.

19) Pearson, R.A., Yee, A.F. *J. of Materials Science*, **1991**, 26, 3828-3844.

20) Lee, J., and Yee, A.F. *Polymer* **2001**, 42, 589–597.

21) Faber, K.T, and Evans, A.G. *ActaMetall* **1983**, 31, 565–576.

22) Faber, and K.T, Evans, A.G. *ActaMetall* **1983**, 31, 577–584.

23) Kawaguchi, T., and Pearson, R.A. *Comp Sci. Technol* **2004**, 64, 1991–2007.

24) Kinloch, A.J., Maxwell, D., and Young, R.J. *J. Mater Sci. Lett*. **1985**, 4, 1276–1279.

25) Rosso, P., Ye, L., Friedrich, K., and Sprenger, S. *J. Appl. Polym. Sci*. **2006**, 100, 1849-1855.

26) Deng, S., Ye, L., and Friedrich, K. J., *Mater. Sci*. **2007**, 42, 2766-2774.